Hindawi
Advances in Civil Engineering
Volume 2019, Article ID 5184287, 10 pages
https://doi.org/10.1155/2019/5184287

Research Article

A Predictive Model of Mining Collapse Extent and Its Application

Jia Nan, Cheng Liu, and Yi Liu

Institute of Public Safety Research, Department of Engineering Physics, Tsinghua University, Beijing 100084, China

Correspondence should be addressed to Yi Liu; liuyi@tsinghua.edu.cn

Received 13 August 2018; Revised 16 October 2018; Accepted 25 October 2018; Published 4 March 2019

Academic Editor: Mario D'Aniello

To reveal the mechanical behavior mechanism of collapse and to control risks effectively, the instability extent of the collapse area was established through theoretical mechanics and numerical methods, taking one metal mine as a case study; on this basis, a routine reinforcement program was determined, and the effect of the program was evaluated. The results show the following. (1) Analytical formulas of the critical slip angle and the collapse height of the ore body were derived by the mechanics method, and the rock mechanics parameters were obtained by field coring and physical and mechanical experiments. The slipping line angle increases along with uniform force Q and is inversely proportional to the bending stiffness. Meanwhile, the calculation formula for the maximum subsidence of ore body was deduced. (2) Numerical results can be used to determine the basic form of the collapse area, and a "U-shaped" collapse area formed when a plastic area passed completely through, resulting in the overall destruction. (3) The grouting reinforcement program includes "determining the instability region ⟶ roadway temporary support ⟶ improve the water environment and surrounding rock bearing capacity ⟶ mining planning" which were determined on the basis of prediction. (4) The hierarchical structure of the rock body and filling were improved combined with the Delphi method, and the grouting effect evaluation model was constructed and verified using the improved FD-AHP method; the evaluation value indicating that the grouting reinforcement improved the bearing capacity of ore body and filling body in collapse area. The research results provide systematic reference and technical support for the analysis of stope collapse mechanism, prediction of hidden trouble, and the subsequent mining.

1. Introduction

Mining safety is an important part of the public safety, and reasonable and effective use of mineral resources is the responsibility of the whole society [1]. With the rapid development of China's social economy, the consumption of mineral resources is also increasing, and high-grade easy-mining mineral resources is increasingly depleting [2]. To meet the demand of economic construction for sustained growth of mineral resources and maintain the steady growth of economic development, under the current technical conditions, for the exploitation of mineral, in addition to continuing to expand to deeper regions, it is necessary to fully recycle the hidden resources caused by the difficult mining or abandoned mining in the early stage of mining [3]. The mining collapse problems bring hidden hazards for the subsequent mining [4]. Prediction of the slip boundary and its influence [5] along with the deformation and subsidence of ore body (filling body) [6] will affect the further exploitation of hidden resources directly.

Facing the extremely complicated mining environment, recovering the hidden resources through determining mining collapse extent, and reinforcement are crucial to mining safety. At present, the main methods to study the instability and collapse of stopes include numerical simulation analysis, catastrophe theory, similar material simulation, and uncertainty method [7–9]. Yao [10], followed by Wood [11], employed the finite element method and the boundary element method to study the conditions and heights of overlying rock collapse caused by stoping. Freidin et al. conducted stress distribution and stability analysis studies on goaf roofs with finite element software and obtained the safe range of underground mining span [12]. Peralta adopted the perturbation method to study the stability of fluid-filled roadways under the influence of mining and analyzed the change pattern of impacts exerted by

different dynamic waves on existing structures. Grig studied the mechanical behaviors of iron ore and marl based on rock mechanics tests with FLAC 2D software [13]. Malan proposed an elastic-viscoplastic method to study the time dependence of creep deformation of the ore rock fault zone during surface excavation works [14]. With respect to stoping of resources with hidden dangers and the countermeasures to hidden dangers, developed countries studied the exploitation of resources containing hidden dangers in underground mines much earlier than China. With a completely different concept being adopted, residual ore was recovered fully and effectively from San Manuel Copper Mine and White Pine Copper Mine in the United States by using the dissolving leaching mining method, which was safe and had low mining cost [15]. Tan et al. studied the stress distribution pattern of semi-U-shaped valley terrains [16].

Before mining of the hidden resources, the most critical step is to determine the influence range of mining stability, especially the location and angle of the slipping line; subsequently, the hidden area can be managed [16]. Meanwhile, there are no general approaches or methods for references [17, 18]. Therefore, to improve mining safety and reveal the mechanical behavior mechanism of collapse and control risks, combined with a metal ore mine as a case study, in view of the complex mining conditions of the collapsed area, the theoretical mechanics and numerical analysis model are built to calculate the influence extent of collapse area through field coring and laboratory physical and mechanical experiments. Based on the rock pressure and rock mechanics theories to predict the sinkage of collapsible ore body, the numerical calculation model was established to verify the shape and the extent of collapsed area. Next, the grouting reinforcement program can be determined, and the effect of the program can be evaluated by the comprehensive evolution FD-AHP method.

Engineering background of the metal mine is as follows. The range of vertical collapse is from elevation −298.3 m to −232.0 m, north-south coordinates from 290.5 to 420.0 (Figure 1), with the width of each stope of approximately 6.5~8 m. The mining has been finished and filled (the remaining stakes are interpillar stope), and the second half of the 0# stope is approximately 22.5 m high. The collapse of the goaf caused the filling of two sides into the goaf and the upper ore body subsidence.

2. Theoretical Prediction Model of the Mining Collapse Extent

2.1. Mechanical Calculation Model of the Slipping Line Angle. Firstly, the theoretical mechanics model with the principle of deletion and simplification is established within the collapse range, where the unit length is taken along the circumference and the radial direction is taken to the boundary of the collapse zone, cutting out a long beam along the axial direction. The line displacement and angular displacement on the side connecting with the mine-out area before collapse are constrained; the constraint can be simplified into a fixed end. The line displacement along the axial displacement on the other side is constrained, and the angle is 0; this

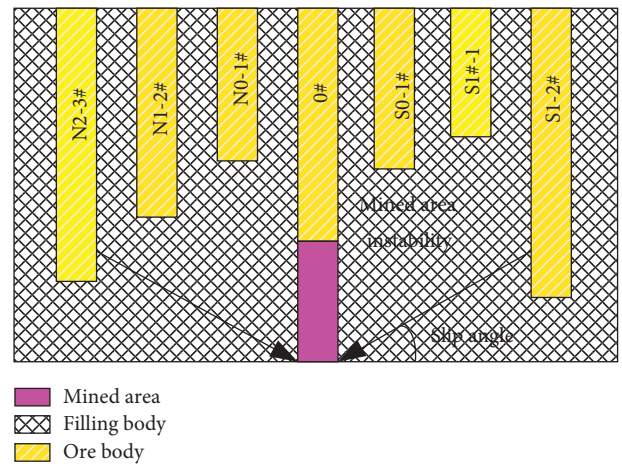

Figure 1: Status of instability collapsed area.

constraint can be simplified as a siding bracket. Suppose that, during the collapse, excavation unloading is evenly distributed. In the simplified stability analysis of beam-column structure, the axial stress and radial stress are the dominant factors that affect the collapse. The tangential stress is the secondary factor, and the tangential stress will affect the geometry of the beam-column structure and physical structure. The mechanical model of the collapse zone can be abstracted as shown in Figure 2.

Then, the rock mass structure within a certain range of the collapse zone can be simplified as a one-time statically indeterminate structure, and the unknown parameters corresponding to the excess unknown force can be solved using the force method, where F indicates axial pressure of the surrounding rock (or filler) in the collapse zone, and Q indicates radial load. As shown in Figure 3, it is assumed that the constraint force on F side is an extra unknown constraint force. By the principle of superposition, we can see that, for the statically indeterminate structure, the mechanical state is the integrated stacking result in the radial uniform force Q and the axial uniform force F (in Figure 4, this mechanical state can be converted into determinate structure in the radial uniform force Q and axial force F).

The bending moment M_0 of any section J can be obtained by the cross section method, as shown in Figure 5 (X-Z coordinate system):

$$M_0 = -F(H - Z) - \frac{Q}{2}(D - x)^2. \tag{1}$$

The mechanical model of the statically indeterminate problem can be established from the approximate differential equation and the boundary condition of the deflection curve:

$$\begin{cases} EIZ'' = -M_0 = \dfrac{Q(D-x)^2}{2} + F(H - Z), \\ Z(0) = 0, Z'(0) = 0, Z(D) = H. \end{cases} \tag{2}$$

The general solution of the differential equation is

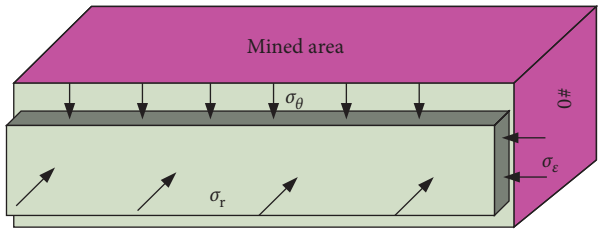

Figure 2: Pillars model of surrounding rock collapse area.

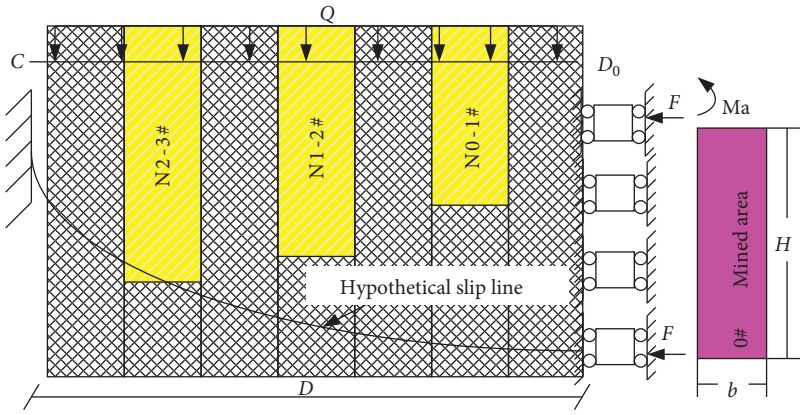

Figure 3: Mechanics model of the collapse region slip line.

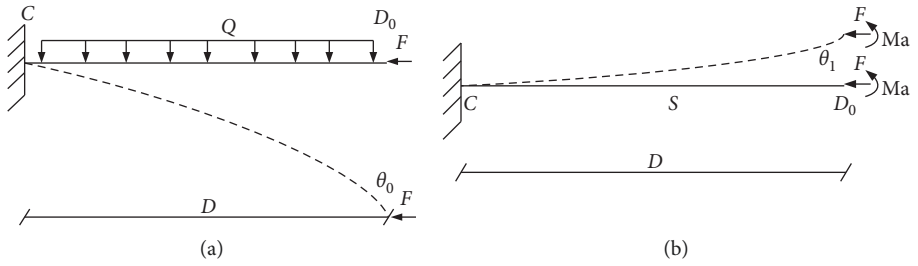

Figure 4: Decomposition of the mechanical state regarding a statically indeterminate structure.

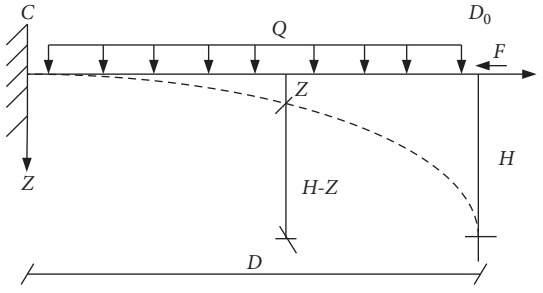

Figure 5: Uniform load.

$$Z_Q = C\cos(Kx) + G\sin(kx) + \frac{\left[k^4H + v^2k^2(D-x)^2 - 2v^2\right]}{k^4}, \tag{3}$$

where H is the maximum deflection. Thus, k, v, C, and G are obtained by the following boundary conditions:

$$\begin{aligned} k^2 &= \frac{F}{EI}, \\ v^2 &= \frac{Q}{2EI}, \\ C &= \frac{\left(2v^2 - k^4H - v^2k^2D\right)}{k^4}, \\ G &= \frac{2v^2D}{k^3}, \\ H &= \frac{QD^4}{8EI}\cdot W_Q(f) = H_0^Q \cdot W_Q(f), \\ f &= kD. \end{aligned} \tag{4}$$

When f tends to be 0, $\lim_{f\longrightarrow 0} W_Q(f) = 1$, the equations of the deflection curve and the corners are as follows:

$$Z_Q = \frac{QD^4}{8EI} \cdot \frac{1}{f}\left[\varphi\cos(kx) + 8f\sin(kx) - \varphi - \frac{8f^2x}{D} + 4\frac{k^2x^2}{D^2}\right],$$
$$\theta_Q = \frac{QD^3}{6EI} \cdot \frac{1}{f^3}\left[6f\cos(kx) + \frac{3}{4}\varphi\sin(kx) - 6f + 6\frac{fx}{D}\right], \tag{5}$$

where

$$\varphi = 8 - 4f^2 - f^4W_Q. \tag{6}$$

Similarly, under the effect of concentration force, $M_0 = -M_{e0} - F(H - Z)$, with the abovementioned curve differential equation and boundary condition, the simplified mechanical model of collapse area are as follows:

$$\begin{cases} EIZ'' = -M_0 = M_{e0} + F(H - Z), \\ Z(0) = 0, Z'(0) = 0, Z(D) = H. \end{cases} \tag{7}$$

However, its general solution can be changed into

$$Z_Q = N\cos(kx) + M\sin(kx) + \frac{[\gamma^2 M_{e0} + k^2 H]}{k^2}, \tag{8}$$

where

$$k^2 = \frac{F}{EI},$$
$$\gamma^2 = \frac{1}{EI}, \tag{9}$$

N and M are integral constants, and H is the maximum deflection; N and M can be obtained from the boundary conditions:

$$N = -\frac{\gamma^2 M_{e0} + k^2 H}{k^2}, \quad M = 0,$$
$$H = \frac{M_{e0}D^2}{2EI} \cdot W_i(k) = H_0^i \cdot W_i(k), \tag{10}$$

where

$$f = kD,$$
$$W_i(f) = \frac{2[1 - \cos(f)]}{f^2\cos(f)}. \tag{11}$$

For $\lim_{f \longrightarrow 0} W_Q(f) = 1$, the solution to the problem becomes

$$Z_i = \frac{M_{e0}D^2}{2EI} \cdot \frac{1}{f^2}\left(2 + f^2W_i\right)[1 - \cos(kx)],$$
$$\theta_i = \frac{M_{e0}D}{EI} \cdot \frac{1}{f}\left(1 + \frac{1}{2}f^2W_i\right)\sin(kx). \tag{12}$$

For the abovementioned statically indeterminate problem, according to the coordination equation, when $x = D$ and $\theta_Q = \theta_i$, M_{e0} can be obtained by the following equation:

$$M_{e0} = \frac{QD^2}{6} \cdot \frac{3f^4W_Q + 12f^2 - 24 + 24fctg(f)}{2f^2\left(2 + f^2W_i\right)}. \tag{13}$$

According to the superposition principle, the deflection curve and the rotation equation are as follows:

$$Z = Z_Q - Z_i = \frac{QD^4}{EI} \cdot \frac{2}{f^3}\left\{\frac{f}{D^2}x^2 - \frac{2fx}{D} + 2\sin(kx) + 2[\cos(kx) - 1]\cot(f)\right\}. \tag{14}$$

The slip angle θ_1 is as follows:

$$\theta_1 = \frac{QD^3}{EI} \cdot \frac{1}{f^2}\left[\frac{x}{D} + \cos(kx) - \cot(f)\sin(kx) - 1\right]. \tag{15}$$

where the Q value is 10.6 MPa, l represents 40 m, E value is 2.7 MPa, I value is 1000, and x value is 8. Substituting the data into the above equations (14) and (15), the slip angle of the collapse zone can be estimated to be 42°.

To obtain the objective calculation parameters of rock mass, the core is obtained from field drilling, and the mechanical parameters of rock are obtained through mechanical experiments and then are transformed into rock physical and mechanical parameters (Figure 6).

It can be concluded that the slipping line angle increases with the increase of uniform force Q and is inversely proportional to the bending stiffness; the slip angle increases with the influence range of the collapse.

2.2. Prediction of Subsidence Displacement of Ore Body. Both sides of mined-out area become unstable due to excavation, and it will enlarge the span of the mined-out area and make the ore body fall. The collapse displacement calculation schematic of mined-out area is shown in Figure 7. The lower half of the shaded area is the falling ore or backfill, the upper half of shaded area is the ore body above the mining area, and the middle part is the hypothetical sinking area. Because the 0# stope in Figure 7 is asymmetrical on both sides, assume the model is tilted. The red square in Figure 7 corresponds to the purple area in Figure 1.

According to the Mohr–Coulomb strength theory [19], A_1 and A_2 are the increased span caused by the instability of the mine-out area, and they can be expressed by the following equation [19]:

$$A_1 = D_k * \tan\alpha + D_k * \cot\left(45^\circ + \frac{\phi}{2}\right),$$
$$A_2 = D_k * \cot\left(45^\circ + \frac{\phi}{2}\right) - D_k * \tan\alpha, \tag{16}$$

where D_k is the thickness of ore body and φ is the internal friction angle of the ore body.

The volume V_a formed after the left body instability in the collapse area is

$$V_a = \frac{D_k * A_1}{2} = \frac{D_k^2 * K_o}{2}\left[\tan\alpha + \cot\left(45^\circ + \frac{\phi}{2}\right)\right]. \tag{17}$$

The volume V_b formed after the right body instability in the collapse area is

(a) (b)

Figure 6: Rock mechanical parameters experiment. (a) Site core test. (b) Mechanical experiment.

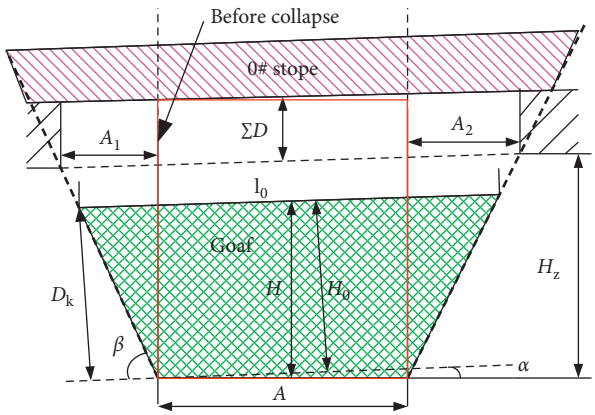

Figure 7: Collapse displacement calculation schematic of the mined-out area.

$$V_b = \frac{D_k * A_2}{2} = \frac{D_k^2 * K_o}{2}\left[\cot\left(45^\circ + \frac{\phi}{2}\right) - \tan\alpha\right]. \quad (18)$$

The volume V_c formed after the collapse of the ore body and filling body in a certain range on the top is

$$\begin{aligned} V_c &= k_d * \sum D * \left(A_1 + \frac{A}{\cos\phi} + A_2\right) \\ &= k_d * \sum\left[\frac{A}{\cos\phi} + 2D_k * \cot\left(45^\circ + \frac{\phi}{2}\right)\right], \end{aligned} \quad (19)$$

where k_d is the expansion coefficient of the ore body and A is the width of the original mined-out area.

Because the fallen ore body and filling body piled into the mined-out area, the pile height H can be obtained by the following three equations:

$$\begin{aligned} V_a + V_b + V_c = \frac{H_0}{2}\left(\frac{A}{\cos\alpha} + l_0\right) \\ + 0.5 * A^2 * \tan\alpha, \end{aligned} \quad (20)$$

$$\frac{H_0}{D_k} = \frac{l_0}{(A_1 + A_2 + (A/\cos\alpha))}, \quad (21)$$

$$H = \frac{H_0}{\cos\alpha} + 0.5A\tan\alpha, \quad (22)$$

$$H_z = \frac{A_2}{2\lambda}\left[A + D_k * \frac{\cos(\beta - \alpha) + \cos(\beta + \alpha)}{\sin\alpha}\right], \quad (23)$$

where l_0 is the oblique width of the top surface of the collapse accumulation body in the mined-out area; H_0 is the height of the collapse accumulation body along the direction of the ore body in the mine-out area; H_z is the total height of the accumulation body in the mine-out area; λ is Poisson's ratio; and β is the collapse slip angle.

Equation (24) can be obtained by simultaneous formulas (20)–(23):

$$H = \frac{\left\{2d_k^2 * k_o * \cot(45^o + (\phi/2)) + 2k_d * \sum D * \left[(A/\cos\alpha) + 2d_k * \cot(45^\circ + (\phi/2))\right] - A^2 * \tan\alpha - (A * d_k/\cos\alpha)\right\}}{\left[2D_k * \cot(45^\circ + (\phi/2)) * \cos\alpha + A\right] + ((A * \tan\alpha)/2)}. \quad (24)$$

Assuming that, the collapsed ore bodies fill the entire mined-out area and make the area to be completely blocked, the necessary condition is as follow:

$$\sum D \geq \frac{d_k^2 (1 - k_o) * \cot(45^o + (\phi/2)) + (D * A/\cos\alpha) + ((A^2 * \tan\alpha)/2)}{[(A/\cos\alpha) + 2D_k * \cot(45^\circ + (\phi/2))](k_d - 1)}. \quad (25)$$

The maximum amount of subsidence of the ore body in the collapse area can be calculated from the above equation:

$$\sum D \geq 4.26\,\text{m}. \quad (26)$$

Therefore, the maximum subsidence of the ore body is related to ore body thickness, internal friction angle, density and dilatancy coefficient, width of the original goaf, ore body inclination angle, and the geometric shape of ore body. The obtained calculation formula can be used as a reference for collapse analysis of similar engineering stopes.

2.3. Numerical Verification Analysis on Collapse Area. The three-dimensional numerical model is established according to the current production map, which is 200 m long, 100 m wide (ore body direction), and 100 m high. In the model, the backfilling waste rock can be simulated using the double yield constitutive model, and the rest are simulated using the Mohr–Coulomb model [20]. The interface between the filling and the backfill is connected by the interface command and uses the complete mesh (187500 units and 199576 nodes were formed in total). Two of the horizontal stresses can be expressed in the form of the pressure coefficient ($\lambda = \nu/1 - \nu$). Meanwhile, rock mass mechanical parameters were obtained by experiment (Table 1).

Based on the results of the inversion calculation, the average elastic modulus is approximately 3.75 GPa, with Poisson's ratio of 0.25, the uniaxial compressive strength of 24 MPa, the proportional limit of 34.6 MPa for the surrounding rock, ore body and filling body with depth of approximately 300 m, the cohesion of 3.6 MPa, the friction angle 36°, the axial horizontal stress of 6.96 MPa, and the vertical stress of 11.2 MPa.

The excavation of the underground space may lead to the destruction of the ore body, with the characteristics of the size of the ore body plastic zone (to avoid size effect, the model is 3 times the size of the model in Figure 1). Figure 8 shows the distribution of the plastic zone formed after the excavation of the 0# stope. The figure reveals that the plastic zone has a wide range of distribution and a plastic zone with the existence of shear and tensile failure. The red outline is the slip line. The plastic zone in the mined-out area roof and both sides expand to the adjacent stope and result in perforation, leading to large-scale instability of the mined-out area. Therefore, it can be known that rib spalling and collapse exist in both sides of the mined-out area because of transverse tension, resulting in the sheeting bodies and collapse along with caving of the roof of various degrees, eventually leading to the instability destruction of the wide area in the mined-out area.

Figure 9 shows the maximum shear strain increment cloud in the state of collapse, revealing that a "U-shaped" collapse area was formed, and the area with the maximum shear strain having the most serious damage.

3. Grouting Reinforcement Measures

In the subsequent stoping works, guaranteed high-quality filling was the precondition for improvements to the lithology of surrounding rocks in the collapse area, whereas the enhanced bearing capacity of the backfill was a key factor for inhibiting the further sinking and destruction of the backfill. Based on the results of numerical analysis, grouting was adopted to improve the strength of the backfill in the U-shaped collapse area effectively, with the overall stability being enhanced. To ensure successful improvements, it was critical to create a better hydrological environment of surrounding rocks in goafs and enhance the self-bearing capacity of these rocks; safe and efficient stoping could be guaranteed by taking timely and effective measures to improve the overall bearing capacity of the backfill. Therefore, the basic principles for controlling surrounding rocks in the collapse area were proposed as follows: (1) pretreatment should be conducted on the water environment in the collapse area; (2) advance prereinforcement should be implemented on the surrounding rocks in goafs; (3) advance support and temporary support should be provided on the ore removal roadway at the bottom; and (4) improvements should be made to the overall stability of the backfill. The overall plan is as shown in Figure 10.

The plastic zone of the surrounding rock has a large range, and its main failure mode was shear failure or shear and tensile comprehensive damage. The bearing capacity of the surrounding rocks could be increased through timely effective grouting reinforcement. Grouting can enhance strength of surrounding rocks and stability of surrounding rocks in future mining practice. Grouting reinforcement was performed on the largest shearing strain cut through belt within the slip line of the unstable collapse area (including crushing zone and plastic zone). Every time after the excavation works were completed, the surrounding rocks in goafs should be filled with high-strength backfill to ensure the development of sufficient bearing capacity, thus, restraining the further sinking and deformation of the surrounding stopes. With respect to the specific grouting situation, as shown in Figure 11, grouting holes were

Table 1: Rock mass mechanical parameters.

Name	Elastic modulus (MPa)	Poisson's ratio	Bulk density (t/m^3)	Cohesion (MPa)	Internal friction angle (°)	Tensile strength (MPa)
Filling body 1	2750	0.19	2.11	0.74	38.0	2.39
Ore body	19760	0.30	3.80	2.45	40.3	2.4
Filling body 2	2080	0.21	2.23	0.56	37.7	1.96

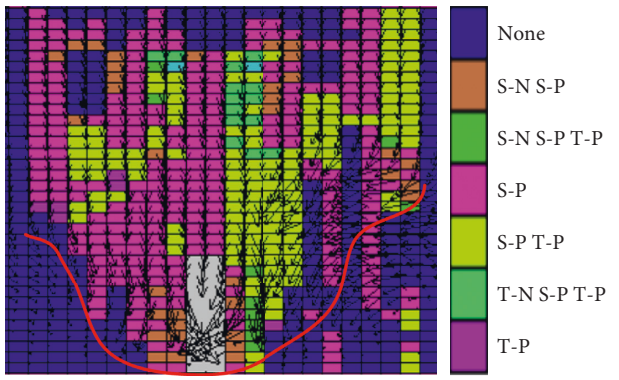

Figure 8: Plastic zone of instability of the mining collapse area.

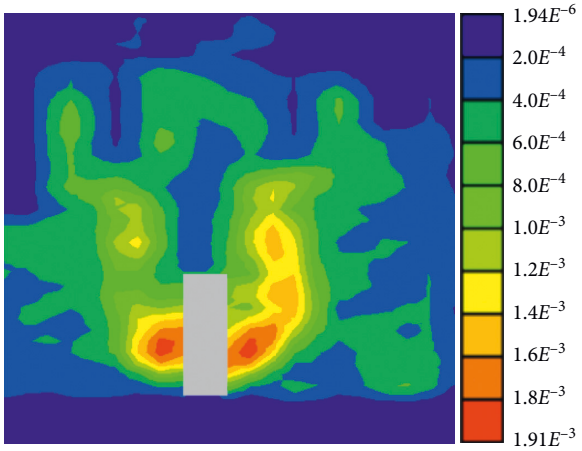

Figure 9: Cloud of the maximum shear strain increment.

arranged in those highly safe drilling chambers outside the collapse area, which were used to detect if the adjacent ore bodies had sunk as well as to block and reinforce the voids and cracks of backfill below the ore bodies, ensuring that the backfill was stable without further collapse in the follow-up stoping works.

4. Inspection Grouting Reinforcement Effects

To judge whether the stope in the collapse area could be safely mined or not, detection of the grouting effects was conducted. In this paper, the grade of ore body and backfill were classified as a multiattribution decision-making problem. Using the combination of the RMR method, BQ method [20], and Delphi group decision-making theory, assessment factors influencing ore bodies and backfill were selected according to the practical situations of stopes, making these factors to be better in line with the uncertainties in the real situation.

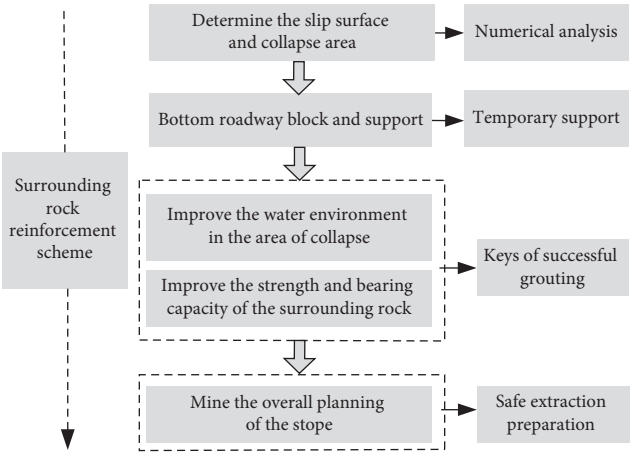

Figure 10: Reinforcement program within the surrounding rock of the hidden area.

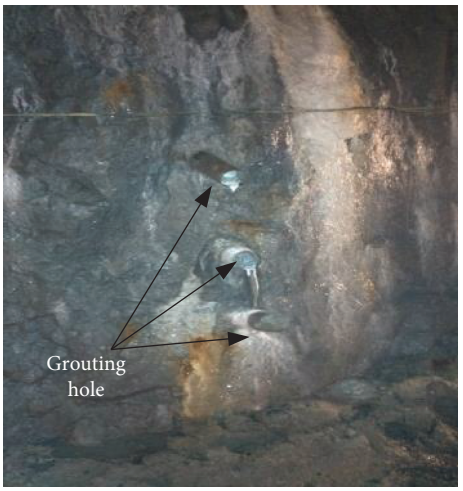

Figure 11: Grouting reinforcement.

Comprehensive analysis of the RMR system and the BQ system revealed that the RMR system did not consider the influences of mechanical parameters, such as fracture and elasticity modulus. However, in the backfill, because of the changes in internal structure of ore body during waste filling and collapse, fractures were formed, greatly changing the mechanical properties of ore body. According to results of a field test, a water pressure test could detect the presence of voids and fractures in the ore body and the backfill. Therefore, the mechanical indices of the BQ system and the results of the water pressure test were included in the classification system as evaluation indices. Meanwhile, no joint spacing existed in the backfill, and it was difficult to

determine the joint spacing because of the engineering environmental conditions. Given this situation, in this paper, regarding the selection of the hierarchical structure to be built, the joint spacing in the RMR system was ignored, with the state of ground stress being considered.

In summary, the following index layers were used in the ore rock and backfill classification method: ① overall rock mass strength; ② rock quality index (RQD); ③ mechanical indexes in the BQ system; ④ results of the water pressure test; and ⑤ state of ground stress. The hierarchical structure model of the ore bodies and the backfill is shown in Figure 12.

The RMR system did not take into consideration water pressure test and elasticity modulus. Currently, there are no uniform domestic and international standards for classifying the results of water pressure tests. Thus, it is necessary to take the existing research into consideration. The principles for classifying the water pressure test evaluation indices were obtained based on field experience, as shown in Table 2.

The fuzzy Delphi analytic hierarchy process (FD-AHP) is a fuzzy group decision-making method combined with fuzzy mathematics appraisal, analytic hierarchy process, and Delphi group decision-making method [21–23]. FD-AHP was used to calculate the total score of rock mass and the backfill; thus, an improved FD-AHP calculation method for the rock mass and the backfill was formed. The basic steps of improved FD-AHP are as follows:

(1) Build a hierarchical structure model to calculate the quality of ore body and backfill, as shown in Figure 12.

(2) Build an AHP hierarchical structural model.

(3) Create a comparison and judgment matrix. For elements on the criterion level, comparison was made one by one. When an element on the above level is taken as the comparison criterion, a comparison scale b_{ij} can be used to express the corresponding criticality of element i and element j on one of these levels.

(4) When the triangular fuzzy number is used to create a group fuzzy judgment matrix, the two-by-two judgment matrix is as follows:

$$b_{ij} = \left[\beta_{ij}\gamma j\delta_{ij}\right], \quad \beta_{ij} \le \gamma_{ij} \le \delta_{ij}, \tag{27}$$

where

$$\begin{aligned} \beta_{ij} &= \min\left(b_{ij\cdot K}\right), \quad K = 1, 2, \ldots, N, \\ \gamma_{ij} &= \text{average}\left(b_{ij\cdot K}\right), \quad K = 1, 2, \ldots, N, \\ \delta_{ij} &= \max\left(b_{ij\cdot K}\right), \quad K = 1, 2, \ldots, N, \end{aligned} \tag{28}$$

where N is the total number of experts giving scores and $b_{ij\cdot K}$ is the corresponding criticality of element i and element j judged by expert K:

$$\text{average}\left(A_1, A_2, \ldots, A_N\right) = \left(A_1 \times A_2 \times \ldots \times A_N\right)^{1/N}. \tag{29}$$

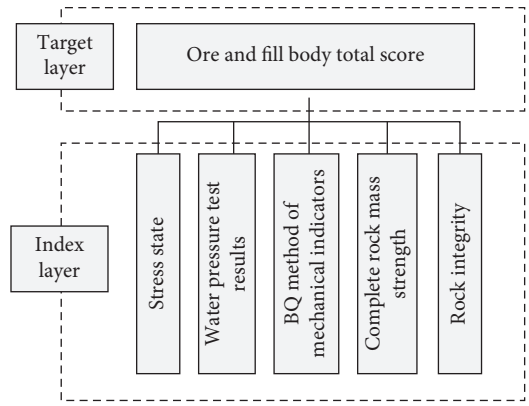

Figure 12: Hierarchical model of the ore body grading and filling.

Table 2: Water pressure test classification.

Qualitative description	LV's value	Rating value
Very good	<10	10
Good	10~20	8
Moderate	20~30	6
Bad	30~40	4
Very bad	>50	2

(5) The group fuzzy weight vector is established based on the group fuzzy judgment matrix b_{ij}, and the corresponding fuzzy weight vector is established using the geometric mean method. The vector is calculated for any evaluation index i ($i = 1, 2, \ldots, m$):

$$R_i = \left(b_{i1} \otimes b_{i2} \otimes \ldots \otimes b_{\text{iM}}\right)^{1/\text{M}}. \tag{30}$$

Through further calculation, the following is obtained:

$$\psi_i = \left(R_1 \oplus R_2 \oplus \ldots \oplus R_M\right)^{-1} \oplus R_i, \tag{31}$$

where $\otimes$ and $\oplus$ are the relationship of triangular fuzzy number multiplication and that of the addition, respectively:

$$\begin{cases} A \oplus B &= \left[A_1 + B_1,\ A_2 + B_2,\ A_3 + B_3\right], \\ A \otimes B &= \left[A_1 \times B_1,\ A_2 \times B_2,\ A_3 \times B_3\right], \\ \dfrac{1}{A} &= \left[\dfrac{1}{A_3}, \dfrac{1}{A_2}, \dfrac{1}{A_1}\right], \end{cases} \tag{32}$$

where

$$\begin{aligned} A &= \left[A_1, A_2, A_3\right], \\ B &= \left[B_1, B_2, B_3\right]. \end{aligned} \tag{33}$$

(6) In weight decision-making analysis, let the fuzzy weight vector of each index be

$$\psi_i = \left(\psi_i^x, \psi_i^z, \psi_i^D\right), \tag{34}$$

where ψ_i^x, ψ_i^z, and ψ_i^D are the minimum, median, and maximum values, respectively, of the three

components of the fuzzy weight vector. The relative weight value of each evaluation index is calculated using the geometrical average approach, with the decision-making weight being obtained through normalization, and the normalized weight vector is

$$\psi_i = \frac{\sqrt[3]{\psi_i^x \times \psi_i^z \times \psi_i^D}}{\sum_i \sqrt[3]{\psi_i^x \times \psi_i^z \times \psi_i^D}}. \quad (35)$$

After normalization, the decision-making weight value of each evaluation index is

$$\begin{aligned} \psi_1 &= 0.15, \\ \psi_2 &= 0.28, \\ \psi_3 &= 0.19, \\ \psi_4 &= 0.12, \\ \psi_5 &= 0.26. \end{aligned} \quad (36)$$

Thus, it is available to calculate the total score F_0 of the classified layers of the ore rock and the backfill based on the evolved FD-AHP, as shown in the following equation:

$$F_0 = \psi_1 M_1 + \psi_2 M_2 + \psi_3 M_3 + \psi_4 M_4 + \psi_5 M_5. \quad (37)$$

Before grouting, the quality improvement score of ore bodies was 81, and that after grouting was 88. Before grouting, the quality improvement score of backfill was 65, and that after grouting was 75. Clearly, the grouting effect was apparent. Based on the above analysis, in the collapse area, with grouting reinforcement, the stress state of the surrounding rock structure was improved; thereby improving the self-bearing capacity of the surrounding rock in the collapse area and the stability of the surrounding rocks to be stoped.

5. Conclusion

(1) According to the structure and force characteristics of the surrounding rock in the collapsed area, the theoretical mechanics model of the influence range of the collapse zone is constructed with the loose circle as the boundary. Meanwhile, based on the force method, the deflection line and the corner equation of a statically indeterminate beam-column of the plastic range are obtained, and the analytic expression of the critical slip angle of the beam-column model is obtained. According to rock physical and mechanical experiments, it can be concluded that the angle of the slip line increased along with the uniform force Q, which is inversely proportional to the bending stiffness; the slip angle increases with the influence range of the collapse.

(2) Based on the theory of mine pressure, rock formation control, and rock mechanics, the basic collapse form of collapse area is analyzed, the calculation formula of collapse height of ore body is derived, and the collapse height of the upper ore body is estimated to be ≥4.26 m. Therefore, the maximum subsidence of ore body is related to ore body thickness, internal friction angle, density and dilatancy coefficients, width of the original goaf, ore body inclination angle, and the geometric shape of ore body. The obtained calculation formula can be used as a reference for collapse analysis of similar engineering stopes.

(3) With the method of numerical analysis, the mechanism of collapse and its catastrophe process are obtained. The influence range of the collapse area is calculated, and the influence range of the collapse area has the form of a "U shape."

(4) The overall grouting reinforcement scheme was determined according to the above analysis results: determine the instability region ⟶ temporary support for laneway ⟶ improve the water environment and the bearing capacity of the surrounding rock ⟶ make mining planning. The safe existing roadways are utilized to layout grouting holes to implement grouting reinforcement in collapse area.

(5) Combined with the field water pressure test, and based on the RMR and BQ methods, the evaluation index of water pressure test results was introduced into the classification method. The hierarchical grading model of ore body and backfill was built, and the improved FD-AHP coupling method was established to evaluate the quality of the filling body before and after grouting. The results show that the quality of the ore body and the filling body was improved obviously, and grouting reinforcement improved the bearing capacity of the ore body and the filling body in the mining collapse area.

Data Availability

The data used to support the findings of this study are available from the corresponding author upon request.

Conflicts of Interest

The authors declare that they have no conflicts of interest.

Acknowledgments

This study was supported by the National Key R&D Program of China (No. 2018YFC0809700) and National Natural Science Foundation of China (Nos. 91646101, 71673158, 91324022, and 91646201).

References

[1] R. Gao, J. Zhang, A. J. S. Spearing, M. Li, B. An, and D. Hao, "Research into stope roof control of compound roof by solid backfilling mining," *International Journal of Mining Science and Technology*, vol. 26, no. 4, pp. 609–614, 2016.

[2] Z.-q. Luo, C.-y. Xie, J.-m. Zhou, N. Jia, X.-m. Liu, and H. Xu, "Numerical analysis of stability for mined-out area in multi-field coupling," *Journal of Central South University*, vol. 22, no. 2, pp. 669–675, 2015.

[3] J. C. Saul, P. J. Evans, and B. C. Forster, "Fault zone architecture and permeability structure," *Geology*, vol. 24, no. 11, pp. 1025–1028, 1996.

[4] T. H. Ma, H. Y. Wang, and G. S. Fu, "Present situation analysis of non-coal mine goaf hazards in China," *Journal of Northeastern University*, vol. 30, no. S1, pp. 91–95, 2009.

[5] K. Guan, W. C. Zhu, L. L. Niu, and Q. Y. Wang, "Three-dimensional upper bound limit analysis of supported cavity roof with arbitrary profile in Hoek-Brown rock mass," *Tunnelling and Underground Space Technology*, vol. 69, pp. 147–154, 2017.

[6] J. L. Peng, J. X. Yang, and M. X. Sun, "Analysis and control on anomaly water inrush in roof of fully-mechanized mining field," *Mining Science and Technology (China)*, vol. 21, no. 1, pp. 89–92, 2011.

[7] R. Hart, P. A. Cundall, and J. Lemos, "Formulation of a three-dimensional distinct element model-Part II. Mechanical calculations for motion and interaction of a system composed of many polyhedral blocks," *International Journal of Rock Mechanics and Mining Sciences & Geomechanics Abstracts*, vol. 25, no. 3, pp. 117–125, 1988.

[8] A. M. Starfield and P. A. Cundall, "Towards a methodology for rock mechanics modelling," *International Journal of Rock Mechanics and Mining Sciences & Geomechanics Abstracts*, vol. 25, no. 3, pp. 99–106, 1988.

[9] D. Mao, B. Nilsen, and M. Lu, "Numerical analysis of rock fall at Hanekleiv road tunnel," *Bulletin of Engineering Geology and the Environment*, vol. 71, no. 4, pp. 783–790, 2012.

[10] X. L. Yao, D. J. Reddish, and B. N. Whittaker, "Non-linear finite element analysis of surface subsidence arising from inclined seam extraction," *International Journal of Rock Mechanics and Mining Sciences & Geomechanics Abstracts*, vol. 30, no. 4, pp. 431–441, 1993.

[11] W. L. Wood and A. Calver, "Lumped versus distributed mass matrices in the finite elements solution of subsurface flow," *Water Resources Research*, vol. 26, no. 5, pp. 819–825, 1990.

[12] A. M. Freidin, S. A. Neverov, A. A. Neverov, and P. A. Filippov, "Mine stability with application of sublevel caving schemes," *Journal of Mining Science*, vol. 44, no. 1, pp. 82–91, 2008.

[13] L. A. Peralta, G. F. Carrier, and C. C. Mow, "An approximate procedure for the solution of a class of transient-wave diffraction problems," *Journal of Applied Mechanics*, vol. 33, no. 1, pp. 168-169, 1966.

[14] D. F. Malan, "Time-dependent behaviour of deep level tabular excavations in hard rock," *Rock Mechanics and Rock Engineering*, vol. 32, no. 2, pp. 123–155, 1999.

[15] W. S. Phillips, D. C. Pearson, C. L. Edwards, and B. W. Stump, "Microseismicity induced by a controlled, mine collapse at white pine, Michigan," *International Journal of Rock Mechanics and Mining Sciences*, vol. 34, no. 3-4, pp. 246.e1–246.e14, 1997.

[16] L. Y. Tan, H. F. Yu, and L. Chen, "A new approach for predicting bedding separation of roof strata in underground coalmines," *International Journal of Rock Mechanics and Mining Sciences*, vol. 61, pp. 183–188, 2013.

[17] F. Q. Liu and J. H. Wang, "A generalized slip line solution to the active earth pressure on circular retaining walls," *Computers and Geotechnics*, vol. 35, no. 2, pp. 155–164, 2008.

[18] F. Q. Liu, J. H. Wang, and L. L. Zhang, "Axi-symmetric active earth pressure obtained by the slip line method with a general tangential stress coefficient," *Computers and Geotechnics*, vol. 36, no. 1-2, pp. 352–358, 2009.

[19] A. Hackston and E. Rutter, "The mohr-coulomb criterion for intact rock strength and friction - a re-evaluation and consideration of failure under polyaxial stresses," *Solid Earth*, vol. 7, no. 2, pp. 493–508, 2016.

[20] H. F. Xu, H. S. Geng, W. D. Li et al., "Theory of strength increment of grouting-reinforced bodies for broken rock mass based on BQ," *Chinese Journal of Geotechnical Engineering*, vol. 49, pp. 1147–1151, 2014.

[21] S.-L. Hsueh, "Assessing the effectiveness of community-promoted environmental protection policy by using a Delphi-fuzzy method: a case study on solar power and plain afforestation in Taiwan," *Renewable and Sustainable Energy Reviews*, vol. 49, no. 6, pp. 1286–1295, 2015.

[22] X. Ying, G.-M. Zeng, G.-Q. Chen, L. Tang, K.-L. Wang, and D.-Y. Huang, "Combining AHP with GIS in synthetic evaluation of eco-environment quality-A case study of Hunan Province, China," *Ecological Modelling*, vol. 209, no. 2, pp. 97–109, 2007.

[23] S. Lee and K.-K. Seo, "A hybrid multi-criteria decision-making model for a cloud service selection problem using BSC, fuzzy delphi method and fuzzy AHP," *Wireless Personal Communications*, vol. 86, no. 1, pp. 57–75, 2015.